Chapter 9

# Carbon Nanotubes: Molecular and Electronic Properties of Regular and Defective Structures

María Leonor Contreras Fuentes and
Roberto Rozas Soto

Additional information is available at the end of the chapter

http://dx.doi.org/10.5772/intechopen.70934

**Abstract**

In this chapter, we describe how structural parameters affect the reactivity of single-walled carbon nanotubes through global reactivity descriptors obtained by the DFT methods (B3LYP/6-31G(d) with real frequencies in all cases). First, we investigate regular *armchair*, *chiral*, and *zigzag* nanotubes with bumpy defects (five- and seven-membered rings), finding that regular and defective *zigzag* nanotubes exhibit the greater conductive ability, reactivity, and capacity of nanotubes to be reduced. The bumpy defects favor those properties with greater intensity in *chiral* nanotubes. We also investigate how the properties of *armchair* nanotubes change in the presence of bumpy, haeckelite, Stone-Wales, and zipper defects, and we found that *armchair* nanotubes with zipper defects show greater reactivity and better conducting abilities enhanced by nitrogen doping and longer nanotubes. In addition, for *armchair* nanotubes containing bumpy defects, our results reveal, considering B3LYP-D3 correction, that bumpy defects confer a greater ability to physically adsorb hydrogen, with adsorption energies of 0.32 eV/adsorbed $H_2$. That value is considered ideal for the reversible adsorption of hydrogen at room temperature and low pressures and therefore favorable for use as a clean energy source. These results contribute to the future design of novel useful materials based in carbon nanotubes.

**Keywords:** nitrogen-doped carbon nanotubes, conceptual DFT, global reactivity descriptors, hydrogen physisorption energy, saturated nanotubes, nanotube chirality, bumpy defects, zipper defects, haeckelite defects, Stone-Wales defects, conductive ability, *armchair*, *chiral*, *zigzag*, dispersion forces

## 1. Introduction

Carbon is a very important chemical element, essential for the existence of multiple types of structures. Organic chemistry, a broad and interesting branch of chemistry, in simple terms, is

defined as carbon chemistry and is closely related, for example, to biochemistry and biomedicine. The understanding of the structure-property relations is an important pillar on which the development of these branches of knowledge is based. Thus, exchanging the position of two groups on a molecule of a recommended drug may mean that it becomes a poison. An example is the case of thalidomide disaster [1] where many babies were born with phocomelia (malformation of the limbs) when R-thalidomide, a compound suitable to mitigate some troublesome symptoms of pregnancy, was administered to their mother but contaminated with its enantiomer (compound with the same mirror image, but not superimposable); moreover, the enantiomer, S-thalidomide, has teratogenic effects.

Carbon nanotubes (CNTs) are a family of compounds that, due to their size, composition, surface ratio, and molecular structure, present useful properties. Being lighter than steel, CNTs have a higher tensile strength. They may also be better conductors than copper [2, 3]. In addition, CNTs can penetrate cell membranes without breaking them [4]. Basic nanotube units are six-membered rings of $sp^2$-hybridized carbon atoms. The diameter of the nanotubes is of great importance in their properties because it modifies the curvature of the surface of the nanotube affecting the distribution of charge density. Also the way these units are arranged, known as chirality of nanotubes, originates conductive or semiconducting nanotubes. It is important to note that here the concept of chirality is not related to the presence of chiral atoms.

Three types of CNTs are known as characterized by the so-called chirality vectors or Hamada indices, as shown in **Figure 1**. CNTs of type (n,n) or *armchair* are metallic; those of type (n,m) or *chiral* and those of type (n,0) or *zigzag* are semiconductors or metallic; *chiral* nanotubes are conductors if the difference n-m is a multiple of 3 [5]. In all these cases, the repeating units are hexagons, and here we call regular CNTs (R) to these nanotubes to differentiate them from other types of CNTs in which there are cyclic units that can be of four, five, seven, or eight members. When present in the nanotubes, these units, different from the hexagons, are known as structural defects. There are different types of structural defects that can be produced by the addition of a pair of carbon atoms. Those having an arrangement (7,5,5,7) are known as bumpy (B) if the defect is repeated in a transverse equidistant form from the ends of the nanotube. If the defect is repeated longitudinally, zipper-type nanotubes (Z) are obtained. **Figure 2** shows the arrangement of nonhexagonal units in some different types of defects. The arrangement (8,4,8,4) represents one of the defects called haeckelite (HK). In addition, the arrangement (5,7,7,5) of the topological defects known as Stone-Wales (SW) is shown. The absence of some atoms (vacancy) or the substitution of some carbon atoms by other elements (doping) is also considered as defects.

The particular structure of the CNTs (mainly the regular ones) can be of a single-wall, SWCNT, or of multiple concentric walls and every day finds new applications in diverse fields of science and technology, and there are a great number of publications and patents which account for it (e.g., see [6–9]). Nanotubes with defects have shown advantages in some fields. For example, doping with nitrogen decreases the toxicity of nanotubes [10] and gives them excellent catalytic properties in oxygen reduction reactions [11, 12]. The bumpy nanotubes present interesting values of hydrogen physisorption energies (0.26 eV/$H_2$), better than similar regular nanotubes, estimated through theoretical studies based on the density functional theory (DFT) [13]. This physisorption energy value is within the suggested ideal range for using hydrogen as a clean

http://dx.doi.org/10.5772/intechopen.70934

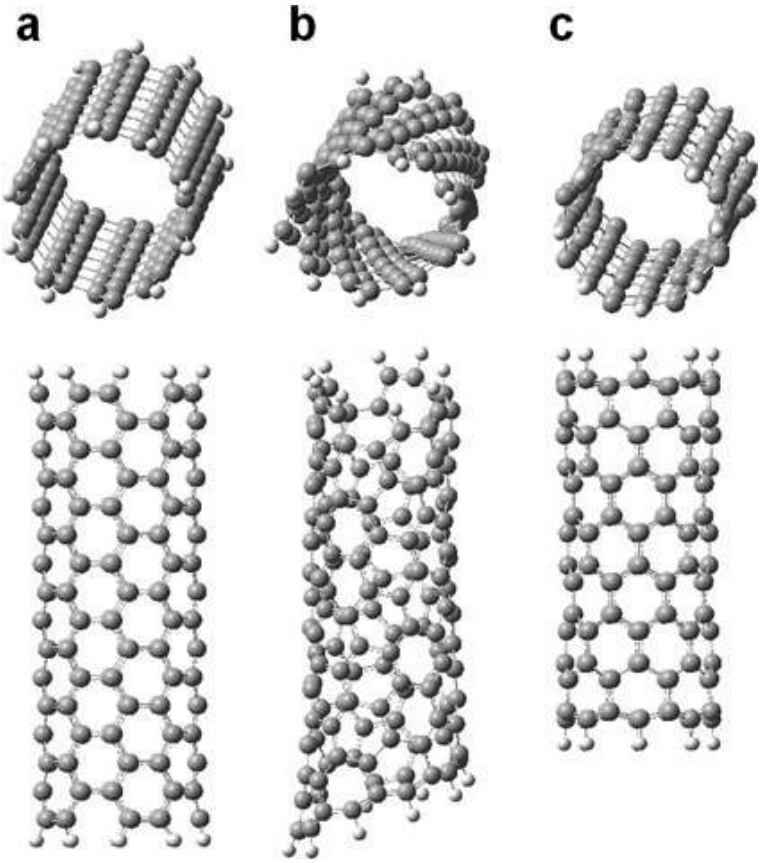


**Figure 1.** Regular nanotube models of different chirality. Perspective and lateral views for (a) *armchair* (5,5), (b) (*chiral* 6,3), and (c) *zigzag* (8,0) nanotube representations.

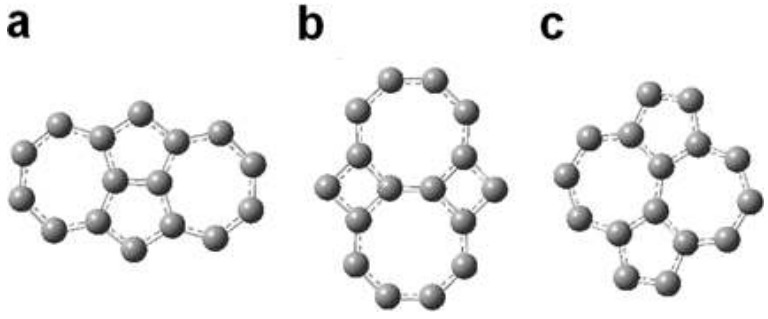


**Figure 2.** Nanotube defects representation. (a) (7,5,5,7) bumpy and zipper defects; (b) (8,4,8,4) haeckelite defect; and (c) (5,7,7,5) Stone-Wales defect.

energy media [14]. The specialized literature lacks enough information to have a broader perspective of the utility and possible applications of defective nanotubes, despite some interesting isolated results [15, 16].

It is therefore interesting and necessary to evaluate how changes in geometric, structural, topological, or doping parameters can affect properties of stability, conductivity, and chemical reactivity of nanotubes and determine if there is any general tendency to predict or modify specifically their behavior in the search for new applications of these advanced materials.

In this chapter, the effects of chirality, chemisorption, number of defects, and the presence of nitrogen on the reactivity of the regular and defective CNTs are analyzed, and results are obtained confirming the good values of hydrogen physisorption energy. This chapter also discusses how the diameter and length of nanotubes, and the presence of nitrogen and the different types of defects (bumpy, haeckelite, Stone-Wales, and zipper) enhance the molecular and electronic properties of CNTs, particularly *armchair*-type, through molecular global descriptors based on the DFT methods.

## 2. Methods

Regular and defective nanotubes are built as finite, open, and terminated by hydrogen atoms by using the HyperTube script [17] embedded in Hyperchem [18]. Saturated nanotubes are full exo-hydrogenated. Nitrogen doping is performed by replacing two carbon atoms by nitrogen atoms at an hexagonal ring building a pyrimidine (with the two nitrogen atoms separated by a carbon atom in the way N1-C2-N3) taking care of locating an additional pyrimidine ring opposite to the first one at the same level in the tube. All the structures are fully optimized by the DFT methods at the B3LYP/6-31G(d) level of theory [19, 20] with Jaguar v9.2 [21]. No symmetry restrictions are applied. Energy minima are verified after the harmonic vibrational frequency real values that are obtained by calculations for optimized structures at the same level of theory. Dispersion forces are corrected by means of the DFT-D3 method [22, 23] validated through the DFT nonlocal method [24] as was performed before [25].

The formation energy, $E_F$, is calculated as follows:

$$E_F = E_{NT} - \sum_{i=1}^{n} n_i E_i \tag{1}$$

where $E_{NT}$ and $E_i$ are the total energy for the nanotube structure (B3LYP/6-31G(d) full optimized) and for the $i$ elements (for instance, C, H, N), respectively; $n_i$ is the number of each element.

The hydrogen physisorption energy, $E_{ph}$, is calculated according to expression (2):

$$E_{ph} = E_{(NT+nH_2)} - E_{NT} - nE_{H_2} + vdW \tag{2}$$

where $E_{(NT+nH_2)}$ and $E_{NT}$ are the total energy for the B3LYP/6-31G(d) full optimized nanotube structure containing the encapsulated hydrogen molecules inside and for the nanotube alone;

$E_{H_2}$ is the total energy for the hydrogen molecule; $n$ is the number of encapsulated hydrogen molecules; and vdW corresponds to the van der Waals interaction correction term accounting for the dispersion forces calculated by DFT-D3 methods [22, 23] as implemented in Jaguar v9.2. Specialized research studies have found B3LYP-D3 as a very accurate method for treating intermolecular interactions [26].

The electronic chemical potential μ is defined [27] as the energy changes of the system with respect to the number of electrons N at a given external potential ν(r) defined by the nuclei:

$$\mu = \left(\frac{\partial E}{\partial N}\right)_{v(r)} \tag{3}$$

After applying the finite difference approximation, the Koopmans theorem [28, 30] and the Kohn-Sham principle [29, 31], global reactivity descriptors are calculated according to Eqs. (4)–(7) for the electronic chemical potential, the chemical hardness η, the global electrophilicity index ω, and the softness S, based on conceptual DFT, respectively [27–34]:

$$\mu = (E_{LUMO} + E_{HOMO})/2 \tag{4}$$

$$\eta = (E_{LUMO} - E_{HOMO})/2 \tag{5}$$

$$\omega = \mu^2/2\eta \tag{6}$$

$$S = 1/\eta \tag{7}$$

where $E_{LUMO}$ and $E_{HOMO}$ are the B3LYP/6-31G(d) energies of the frontier orbitals: the lowest unoccupied molecular orbitals and the highest occupied molecular orbitals, respectively. The bandgap, BG, is calculated as the energy difference between the frontier molecular orbitals $E_{LUMO}-E_{HOMO}$.

## 3. Chirality effect

In this section, we analyze the reactivity of *armchair*, *chiral*, and *zigzag* nanotubes, regular and with bumpy defects, using theoretical DFT methods. We study the effects of both nitrogen doping and the total hydrogenation of nanotubes on the electronic properties.

### 3.1. Bandgap

The bandgap is the energy difference between the conduction band and the valence band. The smaller is the bandgap, the nanotube tends to have better conductive ability. The regular CNTs (defect free) formed only by six-membered ring units exhibit properties that depend on the ordering of the rings in the nanotube or chirality. Studies with the DFT methods at B3LYP/6-31G(d) for CNTs of similar diameters (between 6.3 and 6.8 Å) and eight carbon-atom layer (cl) of length revealed that the bandgap value decreases in the order: *armchair* (5,5) > *chiral* (6,3) > *zigzag* (8,0) with values 1.77, 1.35, and 0.42 eV, respectively [25]. Nitrogen-doped CNTs

(N-CNTs) in the three mentioned cases show a decrease in the bandgap in the order: *chiral*, *armchair*, and *zigzag* with bandgap values of 1.26, 1.16, and 0.0 eV, respectively. Doped and nondoped z*igzag* nanotubes exhibit the smallest bandgap [25].

CNTs with two bumpy defects and similar dimensions than the mentioned regular CNTs show the following order of bandgap: *armchair* > *zigzag* > *chiral* with values of 1.72, 0.43, and 0.31 eV, respectively. In the case of nitrogen-doped CNTs with bumpy defects, obtained bandgap values increase for *zigzag* and *chiral* nanotubes (0.83 and 0.86 eV, respectively), but decreases for *armchair* nanotubes (1.29 eV) (see 1a in **Table 1**). These results indicate that the bumpy defect decreases the bandgap in the doped and nondoped *chiral* nanotubes. In the *zigzag* and *armchair* nanotubes, the bumpy effect depends on the presence of nitrogen since in both nondoped cases, the presence of the bumpy defect does not affect too much, whereas in the cases of doped *zigzag* and *armchair* nanotubes, the presence of the bumpy defect increases the bandgap. *Armchair* nanotubes with five bumpy defects in their structure, doped and nondoped, decrease the bandgap to 1.17 eV (see 1e in **Table 1**).

The hydrogenation of nanotubes with bumpy defects increases the bandgap to levels between 6.12 and 6.57 eV for two bumpy defects and between 6.37 and 6.79 eV for five bumpy defects. This behavior is expected due to the $sp^3$ hybridization that makes the structures of the nanotubes similar to each other with a similar electron density distribution (see 2a and 2e in **Table 2**). In all cases, it can be observed that nitrogen decreases the bandgap with values between 5.46 and 5.83 eV.

In other words, in terms of conductive ability, our calculations reveal that both regular and bumpy nanotubes show the same trend: *zigzag* and *chiral* nanotubes have higher conductive

| Entry | Reactivity descriptor | Armchair | | Chiral | | Zigzag | |
|---|---|---|---|---|---|---|---|
| | | 0 N | 4 N | 0 N | 4 N | 0 N | 4 N |
| **with two bumpy defects** | | | | | | | |
| 1a | BG | 1.72 | 1.29 | 0.31 | 0.86 | 0.43 | 0.83 |
| 1b | μ | −3.67 | −3.25 | −3.67 | −3.33 | −3.49 | −3.48 |
| 1c | η | 0.86 | 0.64 | 0.16 | 0.43 | 0.21 | 0.41 |
| 1d | ω | 7.82 | 8.19 | 43.22 | 12.83 | 28.52 | 14.66 |
| **with five bumpy defects** | | | | | | | |
| 1e | BG | 1.17 | 1.17 | | | | |
| 1f | μ | −3.65 | −3.64 | | | | |
| 1g | η | 0.59 | 0.58 | | | | |
| 1h | ω | 11.35 | 11.32 | | | | |

**Table 1.** B3LYP/6-31G(d) bandgap ($E_{LUMO}-E_{HOMO}$), BG, electronic chemical potential, μ, chemical hardness, $\eta$, and global electrophilicity, $\omega$, in eV, for a series of 32 nitrogen-doped and nondoped *armchair* (5,5), *chiral* (6,3), and *zigzag* (8,0) bumpy nanotubes, with two and five bumpy defects, all of them having a similar diameter (6.3–6.7 Å) and 8 cl of length.

| Entry | Reactivity descriptor | Armchair | | Chiral | | Zigzag | |
|---|---|---|---|---|---|---|---|
| | | 0 N | 4 N | 0 N | 4 N | 0 N | 4 N |
| **with two bumpy defects** | | | | | | | |
| 2a | BG | 6.29 | 5.56 | 6.12 | 5.62 | 6.57 | 5.46 |
| 2b | μ | −2.71 | −2.10 | −2.71 | −2.21 | −2.71 | −1.82 |
| 2c | η | 3.14 | 2.78 | 3.06 | 2.81 | 3.28 | 2.73 |
| 2d | ω | 1.17 | 0.79 | 1.20 | 0.87 | 1.12 | 0.61 |
| **with five bumpy defects** | | | | | | | |
| 2e | BG | 6.53 | 5.83 | 6.37 | 5.79 | 6.79 | 5.48 |
| 2f | μ | −2.73 | −2.28 | −2.75 | −2.32 | −2.88 | −2.04 |
| 2g | η | 3.27 | 2.92 | 3.19 | 2.90 | 3.39 | 2.74 |
| 2h | ω | 1.14 | 0.89 | 1.18 | 0.93 | 1.22 | 0.76 |

**Table 2.** B3LYP/6-31G(d) bandgap ($E_{LUMO}-E_{HOMO}$) BG, electronic chemical potential μ, chemical hardness η, and global electrophilicity index ω, in eV, for a series of *hydrogenated* nitrogen-doped and nondoped *armchair* (5,5), *chiral* (6,3), and *zigzag* (8,0) nanotubes, with two and five bumpy defects, all of them having a similar diameter (6.3–6.7 Å) and 8 cl of length.

abilities than *armchair* nanotubes. The incorporation of bumpy defects in nanotubes only increases the conductive ability of *chiral* nanotubes (doped or nondoped). Nitrogen doping increases the conductive ability of the three types of regular nanotubes and that of the *armchair* nanotubes with two bumpy defects.

### 3.2. Chemical potential

The chemical potential μ, is the inverse of electronegativity. It measures the tendency of electrons to escape from an equilibrium system. At higher value of the chemical potential, the molecule behaves as a better electron-donor against an acceptor. In a study of diene and dienophile reactivity in Diels-Alder reactions in the context of conceptual DFT at the B3LYP/6-31G(d) level, a compound with μ = −1.85 eV was characterized as electron-donor while another compound with μ = −7.04 eV was considered as electron-acceptor [34].

The values of μ for the regular *armchair*, *chiral*, and *zigzag* nanotubes determined at the same level of theory fluctuate between −3.57 and −3.06 eV. The values of μ for the corresponding nitrogen-doped and nondoped nanotubes with two bumpy defects decrease to −3.67 and −3.25 eV, respectively (the only exception is exhibited by nondoped *zigzag* nanotubes with a μ value of −3.49 eV) and also decrease for *armchair* nanotubes with five defects (see 1b and 1f in **Table 1**). Nitrogen doping slightly increases the value of μ. That means, there is not a very marked difference of chemical potential for nanotubes of different chirality, with or without bumpy defects, doped or nondoped defects. The values of μ are intermediates between the electron-donors and the electron acceptors leaving open the potentiality to behave as electron-donors or electron acceptors.

In the saturated nondoped nanotubes, μ increases to values of −2.88 to −2.71 eV and in the presence of nitrogen doping, μ increases to −1.82 eV being the *zigzag* nanotubes the ones with the greater value of μ (see 2b and 2f in **Table 2**) and likely with a higher ability to be oxidized. Therefore, *zigzag* saturated nitrogen-doped nanotubes could potentially behave as a catalyst in C-H activation reactions [12].

### 3.3. Hardness

The hardness, η, is a useful reactivity descriptor associated to the resistance of a molecule to exchange electronic density with the environment [27, 34]. It measures the stability of a system. The increase of η is normally associated with a stabilizing process having a negative change of energy.

In the regular nanotubes, η increases in the order: *zigzag* (8,0) > *chiral* (6,3) > *armchair* (5,5), with η values of 0.21, 0.68, and 0.89 eV, respectively, determined at B3LYP/6-31G(d) [25]. When regular *zigzag*, *chiral*, and *armchair* nanotubes are nitrogen-doped, η decreases to values of 0.20, 0.63, and 0.58 eV, respectively [25].

Defective nanotubes exhibit a decrease in η values. The only exception is for doped *zigzag* nanotubes. *Armchair* nanotubes with two bumpy defects reveal the highest values of η (0.64 and 0.86 eV for nitrogen-doped and nondoped nanotubes, respectively) compared to *chiral* and *zigzag* nanotubes with η values between 0.16 and 0.43 eV including nitrogen-doped and nondoped systems. Nitrogen doping increases η in *chiral* and *zigzag* nanotubes, but decreases it in *armchair* nanotubes with two defects. In the *armchair* nanotubes with five defects, η decreases also (0.59 eV) unaffected by the presence of nitrogen doping (see 1c and 1g in **Table 1**). That is, η depends on the chirality. Regular *zigzag* nanotubes are the most reactive. Bumpy defects increase the reactivity of nanotubes (with the exception of doped *zigzag* and *armchair* nanotubes). Nitrogen doping also increases the reactivity of regular nanotubes especially the *armchair* nanotubes and also increases the reactivity of *armchair* nanotubes with bumpy defects. The increase in the number of bumpy defects increases the reactivity of the *armchair* nanotubes.

The saturated nanotubes with two bumpy defects do not show large η differences with chirality (3.06–3.28 eV) nor is it affected too much in nanotubes with five bumpy defects (3.19–3.39 eV). In all cases, nitrogen doping makes η decrease (2.73–2.92 eV) (see 2c and 2 g in **Table 2**) and consequently, increases nanotube reactivity.

### 3.4. Electrophilicity index

The electrophilicity index ω, as a descriptor of molecular reactivity, gives a measure of the stabilizing energy of a molecule when it acquires some additional amount of electron density from the environment. The value of ω allows to differentiating the power of the molecules that act as electrophiles. Thus, for organic compounds, strong electrophiles are considered to have ω > 1.5 eV and weak electrophiles have ω < 0.8 eV [35]. According to this classification, the CNTs are strong electrophiles since they exhibit ω values that are much higher than 1.5 eV. Also, a higher value of ω may be associated with a greater trend of the compound to be reduced due to its ability to acquire electronic density.

The values of ω for the regular nanotubes were reported to be dependent on chirality and grow in the order: *armchair* (5,5) < *chiral* (6,3) < *zigzag* (8,0), with values of ω of 6.56, 9.42, and 28.43 eV, respectively. Nitrogen doping slightly decreases the ω value in the *armchair* (6.42 eV) and *chiral* (8.46 eV) nanotubes while increases the ω value in *zigzag* nanotubes (30.07 eV) [25]. The bumpy defects increase the value of ω especially in *chiral* nanotubes (43.22 eV). The *armchair* nanotubes with two bumpy defects are the ones with the lowest value of ω (7.82 eV), which rises in nanotubes with five bumpy defects (11.35 eV). Nitrogen-doped nanotubes exhibit lower ω values with the only exception of *armchair* nanotubes with two bumpy defects (8.19 eV) (see 1d and 1h in **Table 1**).

The saturated nanotubes with two and five bumpy defects, independent of the chirality, decrease the values of ω (1.12–1.22 eV). For the nitrogen-doped nanotubes, the value of ω is even lower (0.61–0.93) with values in the range of the weak electrophiles (see 2d and 2h in **Table 2**).

Detailed analysis of the results obtained for this group of regular and bumpy defective nanotubes (with 8 cl of length) reveals that the *zigzag* nanotubes are those that exhibit greater conductive ability. Also the *zigzag* nanotubes are the most reactive and exhibit a great capacity to be reduced, to acquire electronic density, or to be strong electrophiles. The *armchair* nanotubes are at the other end. The presence of nitrogen in *armchair* regular nanotubes increases their conductive ability. The presence of bumpy defects also enhances their reactivity and their ability to be reduced, especially with five bumpy defects. Bumpy defects, in general, increase the conductivity, the reactivity, and the capacity of nanotubes to be reduced, with greater intensity in the *chiral* nanotubes.

The 8 cl saturated nanotubes, regular and with bumpy defects, exhibit a significant decrease in conductive ability counteracted by the presence of nitrogen. Our calculations reveal that they are less reactive and their ability to acquire electronic density or to behave as electron acceptors decreases when compared to unsaturated nanotubes with a quite good consistence within the different reactivity descriptors.

## 4. Hydrogen adsorption for the carbon nanotubes with defects

Inspired by the unique properties of nanotubes and driven by the idea of contributing to a clean energy source for vehicular use, several authors have studied the possibility of using CNTs as hydrogen transporters [36–40]. Hydrogen may be chemisorbed (covalently attached to carbon atoms) or physisorbed (adsorbed as molecular hydrogen through noncovalent interactions with the nanotube). The results have generated controversy since they have not been reproducible [41, 42]. A reasonable explanation is probably due to the presence of uncontrolled defects in the nanotube that make vary the curvature of the nanotube, the electronic density distribution, and therefore its properties [43]. For example, (7,5,5,7) SW defects increase the ability to adsorb $H_2$ of the *armchair* (5,5), whereas (5,7,7,5) SW defects decrease the ability to adsorb $H_2$ of these nanotubes as was established using the DFT methods at the B3LYP/LanL2DZ level [44]. Additionally, the number of defects in the nanotube affects the reactivity [44]. Other

DFT studies for *armchair* (10,10) nanotubes show that SW defects with five- and eight-membered rings have a greater ability to adsorb $H_2$ than SW defects with five- and seven-membered rings [43], which is also valid for nanotubes of different chirality [43, 45].

SW defects have also been studied in relation to metal-decorated nanotubes and their effects on hydrogen adsorption [46, 47] and also in the study of the interactions with metallic particles and ions [48]. The results obtained for *armchair* (6,6) nanotubes with SW defects at the B3LYP/6-31G(d) level focus on the charge transfer to ions and their relation to the electromigration where the SW defects facilitate the migration of positively charged ions ($In^+$ and $In^{3+}$) through the nanotube [48].

In relation to hydrogen storage as a potential source of clean energy, one requirement is to achieve that at least 5.5 wt% of hydrogen [49] can be released under ambient pressure and temperature conditions. For achieving that goal and to favor a reversible $H_2$ adsorption-desorption process, it is required that the interaction energy CNT-$H_2$ be of the order of 0.1–0.5 eV/$H_2$, according to calculations of first principles and to thermodynamic considerations [14, 39, 50, 51].

Hydrogen chemisorption energy is a chirality-dependent exothermic property. *Zigzag* nitrogen-doped and nondoped nanotubes reveal as the most exothermic followed by the *chiral* and *armchair* nanotubes [25]. On the contrary, hydrogen physisorption energies, $E_{ph}$, exhibit endothermic values. $E_{ph}$ values for saturated, nitrogen-doped *armchair* CNTs obtained by the DFT [B3LYP/6-31G(d)] methods are within the ideal mentioned range (0.26 eV/$H_2$ for 12 $H_2$ physisorbed into a (4,4) nanotube) and grow for *chiral* and *zigzag* nitrogen-doped nanotubes [25] in excellent agreement with results obtained for *armchair*, *chiral*, and *zigzag* CNTs by means of the DFT methods that use the local density approximation [37]. In addition to the chirality, the diameter and length of the nanotube affect the nanotube-$H_2$ interactions. The diameter changes cause the variation in the nanotube curvature affecting the arrangement of the molecular orbitals [4], and the nanotube length variation affects the diffusivity as was determined for drug adsorption [52]. $E_{ph}$ values decrease for nanotubes with a smaller diameter and a larger length (higher number of carbon-atom layers) but increase with the number of adsorbed $H_2$.

Bumpy defects and nitrogen doping favor interaction with nanotube-$H_2$. Saturated *armchair* (4,4) nitrogen-doped nanotubes with bumpy defects and 20 cl of length can encapsulate 15 $H_2$ molecules ($C_{164}N_4H_{210}$ stoichiometry) with a favorable $E_{ph}$ of 0.11 eV/$H_2$ obtained at the B3LYP/6-31G(d) level [13]. Our calculations, considering dispersion forces correction, reveal that saturated nondoped *armchair* (5,5) nanotubes with bumpy defects and 16 cl of length can encapsulate 44 $H_2$ molecules (stoichiometry $C_{170}H_{278}$) with a good $E_{ph}$ value of 0.32 eV/$H_2$. **Figure 3** shows the optimized structure of this system having a hydrogen content of 12 wt%.

The actual available experimental and theoretical information related to hydrogen adsorption in nanotubes indicates that the structural effects that allow obtaining hydrogen physisorption energies within the range considered ideal for the reversible storage of hydrogen (0.1–0.4 eV/$H_2$ under environmental conditions) are those that favor the nanotube-$H_2$ electrostatic interactions. Parameters such as the chirality of the nanotube, a suitable diameter and length, and the

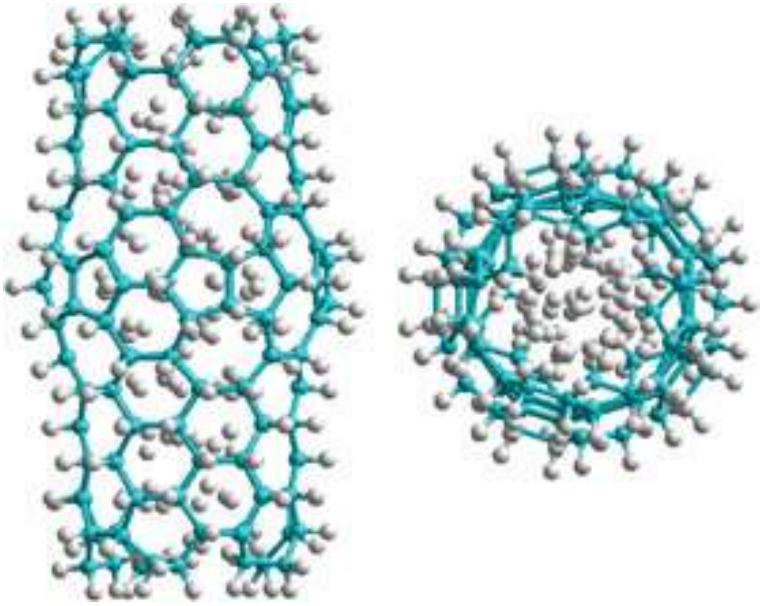

**Figure 3.** B3LYP/6-31G(d) fully optimized structure of an hydrogenated *armchair* (5,5) bumpy, nondoped nanotube, with 16 cl of length having adsorbed 44 hydrogen molecules (stoichiometry $C_{170}H_{278}$; Eph = 0.32 eV/$H_2$). Front and lateral views.

presence of defects that generate suitable spaces, as explained above, can be predicted through DFT calculations. However, the use of conceptual DFT reactivity descriptors (μ, η, ω, and S) to correlate or predict hydrogen physisorption energies in nanotubes is not viewed as adequate. Their use is related and manifests mainly in molecular interactions in which there is charge transfer wherein nucleophiles, electrophiles, or species that change their oxidation state take part. A correlation of these descriptors with the hydrogen adsorption efficiency in nanotubes, at this time, could only have limited validity and provided it is used in conjunction with other descriptors such as diameter, length, number of defects, or others to be set.

## 5. Armchair nanotubes

Nitrogen-doped *armchair* nanotubes are expected to be good catalysts for oxygen reduction reactions compared to their *chiral* and *zigzag* nanotubes because of their particular distribution of electric charge [12, 25]. In this section, we analyze the effect of different types of defects in the reactivity of *armchair* structures by using global descriptors based on the DFT methods. Bumpy, haeckelite, Stone-Wales, and zipper defects are considered (see **Figure 4**). We also analyze the effects of nitrogen doping, the diameter and length of the nanotubes, the number of defects and the charges on the carbon atom adjacent to the two pyrimidine nitrogen atoms.

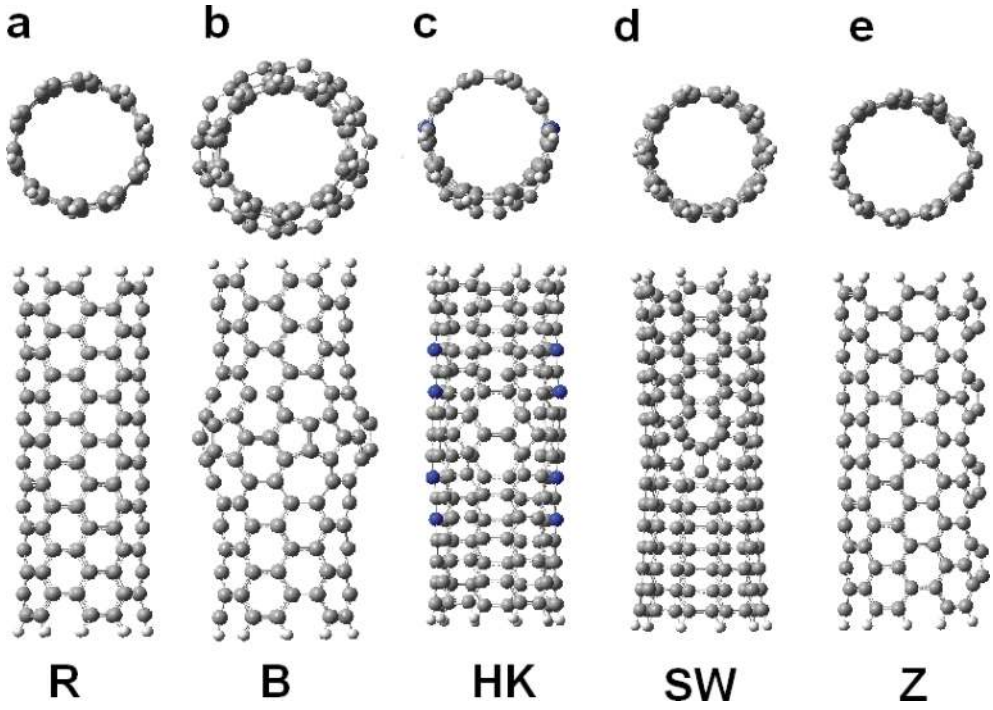


**Figure 4.** B3LYP/6-31G(d) fully optimized *armchair* (5,5) nanotube structures. Front and lateral views showing (a) regular R; (b) bumpy B, with five defects; (c) haeckelite HK, with one defect doped with eight nitrogen atoms; (d) Stone-Wales SW, with one defect; and (e) zipper Z, with four defects, nanotubes with 16 cl of length each.

### 5.1. Formation energies

Nitrogen-doped *armchair* nanotubes in all cases show higher values of $E_F$ than nondoped nanotubes, indicating a greater reactivity. The $E_F$ values are calculated according to Eq. (1). A lower value of $E_F$ indicates greater stability. Bumpy nanotubes are the most reactive. Reactivity also increases as the number of defects in the nanotube increases as shown in **Table 3** for 16 cl *armchair* nanotubes (see 3b and 3c). The corresponding stoichiometry is also shown in **Table 3**. Regular nanotubes with smaller diameter are more reactive than those with larger diameter and exhibit $E_F$ values of −0.72 and −1.26 eV, respectively. Defective nanotubes reveal the same trend. For instance, the *armchair* (5,5) and (6,6) nanotubes, both with one bumpy defect exhibit $E_F$ values of −0.67 and −1.18 eV, respectively. The same trend is shown for the *armchair* (5,5) and (6,6) nanotubes with one SW defect (see 3d and 3h in **Table 3**).

### 5.2. Bandgap and chemical potential

Three groups of *armchair* nanotubes were studied: (1) (5,5) with 16 cl of length (see **Table 4**); (2) (6,6) with 16 cl of length (see **Figure 5**); and (3) (5,5) with 20 cl of length (see **Figure 6**) with bandgap values between 0.54 and 1.27 eV.

| Entry | Type | $E_F$ | | Stoichiometry | |
|---|---|---|---|---|---|
| | | 0 N | 4 N | 0 N | 4 N |
| 3a | (5,5)-R-16 cl | −0.72 | −0.51 | C160H20 | C156N4H20 |
| 3b | (5,5)-B-1D-16 cl | −0.67 | −0.45 | C162H20 | C158N4H20 |
| 3c | (5,5)-B-5D-16 cl | −0.31 | −0.13 | C170H20 | C166N4H20 |
| 3d | (5,5)-SW-1D-16 cl | −0.59 | −0.38 | C160H20 | C156N4H20 |
| 3e | (5,5)-Z-16 cl | −0.57 | −0.39 | C168H20 | C164 N4H20 |
| 3f | (6,6)-R-16 cl | −1.26 | −1.03 | C192H24 | C188N4H24 |
| 3g | (6,6)-B-1D-16 cl | −1.18 | −0.95 | C194H24 | C190 N4H24 |
| 3h | (6,6)-SW-1D-16 cl | −1.14 | −0.92 | C192H24 | C188N4H24 |

**Table 3.** B3LYP/6-31G(d) formation energy $E_F$, in eV, and stoichiometry, for some nitrogen-doped and nondoped *armchair* (5,5) and (6,6) regular, bumpy (with one and five defects), Stone-Wales (with one defect), and zipper nanotubes, all of them having 16 cl of length.

| Entry | Type | BG | μ | η | ω | S |
|---|---|---|---|---|---|---|
| 4a | R-0N | 1.13 | −3.57 | 0.56 | 11.32 | 0.89 |
| 4b | R-4N | 0.85 | −3.31 | 0.42 | 12.92 | 1.18 |
| 4c | B-1D-0N | 1.15 | −3.62 | 0.57 | 11.39 | 0.87 |
| 4d | B-1D-4N | 0.76 | −3.28 | 0.38 | 14.18 | 1.32 |
| 4e | B-5D-0N | 0.89 | −3.72 | 0.45 | 15.52 | 1.12 |
| 4f | B-5D-4N | 0.67 | −3.45 | 0.34 | 17.71 | 1.49 |
| 4g | SW-1D-0N | 0.49 | −3.54 | 0.24 | 25.78 | 2.06 |
| 4h | SW-1D-4N | 0.83 | −3.20 | 0.41 | 12.43 | 1.21 |
| 4i | Z-0N | 1.05 | −3.97 | 0.53 | 15.00 | 0.95 |
| 4j | Z-4N | 0.82 | −3.72 | 0.41 | 16.86 | 1.22 |

**Table 4.** B3LYP/6-31G(d) bandgap ($E_{LUMO}$-$E_{HOMO}$) BG, electronic chemical potential μ, chemical hardness η, and global electrophilicity index ω, in eV, and softness S, in 1/eV, for a series of nitrogen-doped and nondoped *armchair* (5,5) regular, bumpy, Stone-Wales, and zipper nanotubes, all of them having 16 cl of length.

Nitrogen doping increases the CNTs conductive ability both in the regular and defective structures, revealing smaller bandgap values for the nitrogen-doped nanotubes than for the nondoped ones. Defects also increase the conductive ability of *armchair* nanotubes. In the nitrogen-doped (5,5) nanotubes, with 16 cl and 20 cl of length, the zipper nanotubes exhibit the best conductive properties (see 4j in **Table 4** and **Figure 6**) with bandgap values of 0.82 and 0.57 eV, respectively. This behavior of the zipper nanotubes was also observed in doped nanotubes of 8 cl as indicated above with a bandgap value of 0.83 eV (see 1a in **Table 1**). As can be appreciated from the obtained values, increasing the length of the nanotubes increases the nanotube conductive ability.

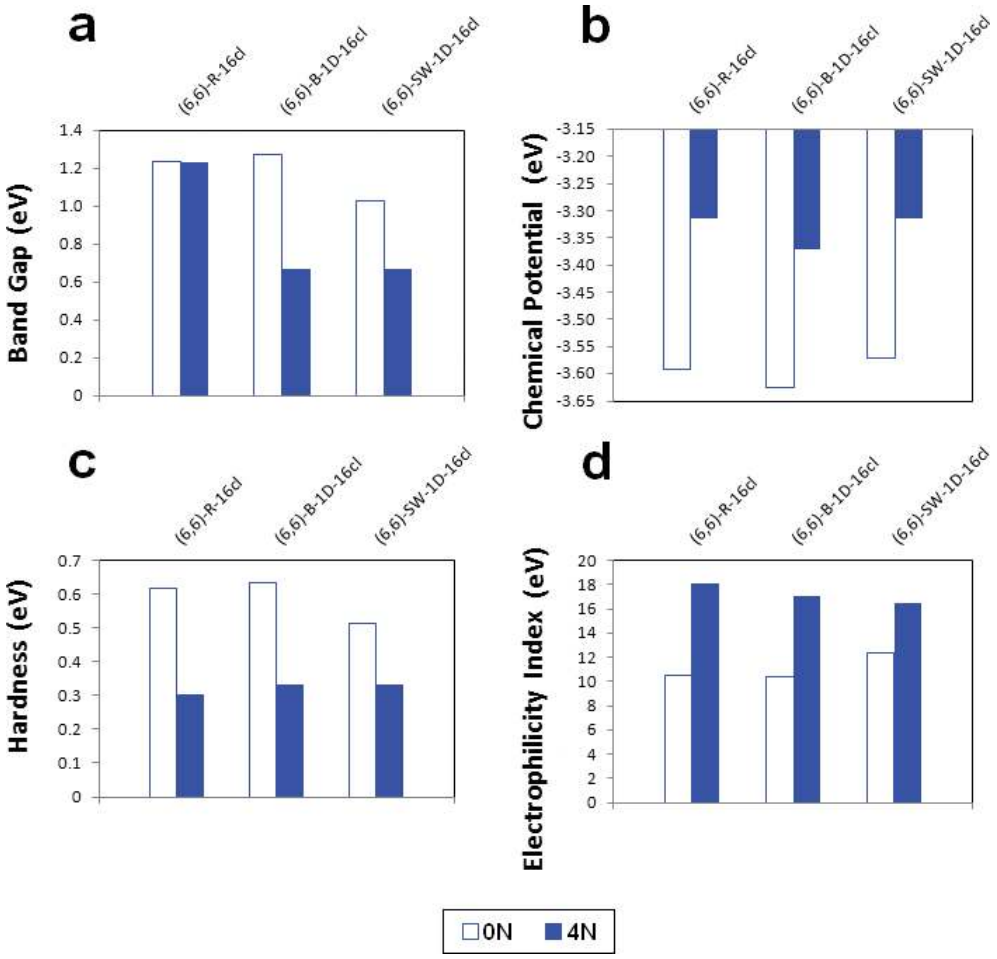


**Figure 5.** B3LYP/6-31G(d) values of (a) bandgap ($E_{LUMO}-E_{HOMO}$); (b) electronic chemical potential; (c) chemical hardness; and (d) global electrophilicity index, for nitrogen-doped and nondoped *armchair* (6,6) regular nanotubes, and *armchair* (6,6) defective nanotubes containing one bumpy defect and one Stone-Wales defect, all of them having 16 cl of length.

Chemical potential of the studied nanotubes presents small variations, with values ranging from −3.20 to −3.97 eV. Nitrogen doping, slightly increases the chemical potential of regular and defective *armchair* nanotubes, for the three groups of *armchair* nanotubes, thereby increasing the electron-donor ability of the doped nanotubes, which is consistent with the nitrogen atom electronic characteristics.

### 5.3. Hardness and softness

The presence of defects decreases the hardness of the (5,5) nanotubes making them more reactive. Nitrogen doping also decreases the hardness of the (5,5) and (6,6) nanotubes of 16 cl,

http://dx.doi.org/10.5772/intechopen.70934

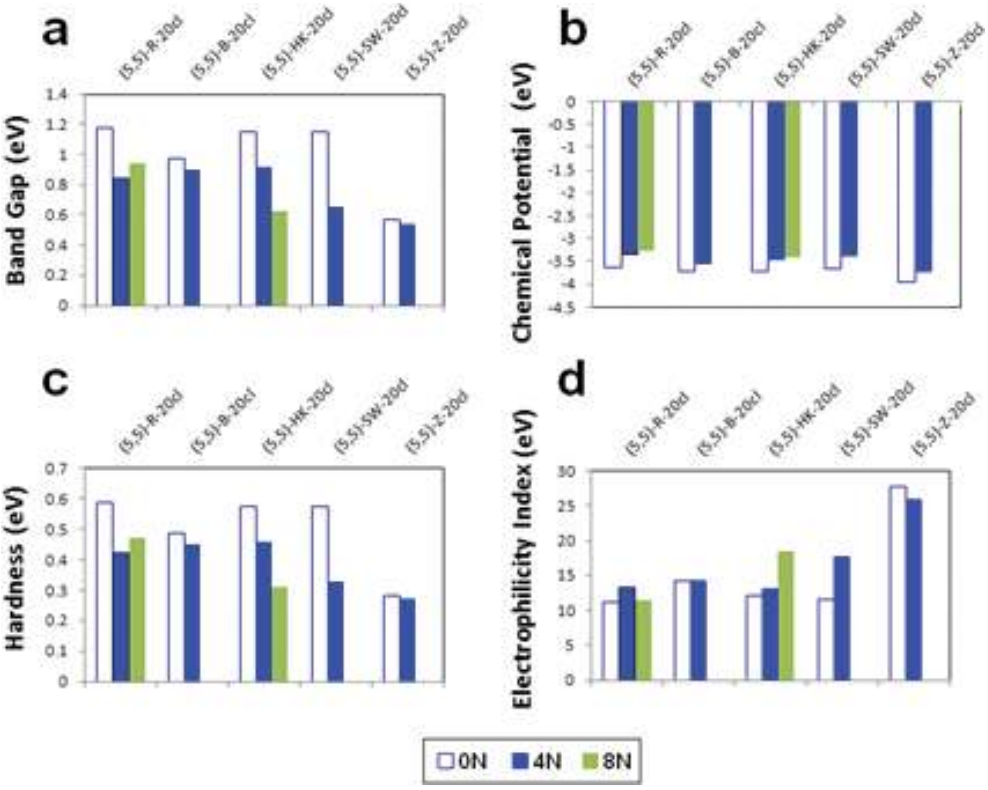


**Figure 6.** B3LYP/6-31G(d) values of (a) bandgap ($E_{LUMO}-E_{HOMO}$); (b) electronic chemical potential; (c) chemical hardness; and (d) global electrophilicity index, for some nitrogen-doped and nondoped *armchair* (5,5) regular, bumpy, haeckelite, Stone-Wales, and zipper nanotubes, all of them having 20 cl of length.

with the exception of (5,5) nanotubes with one SW defect (see 4h vs. 4g in **Table 4**). For the (5,5) nanotubes of 20 cl, the same previous trends are maintained without exceptions (see **Figure 6**). Nitrogen-doped zipper-defected (5,5) nanotubes of 20 cl are predicted to be the most reactive with a hardness of 0.28 eV. They are more reactive than nitrogen-doped zipper-defected (5,5) nanotubes of 16 cl with a value of hardness of 0.41 eV (see 4j in **Table 4**). The effect of nitrogen doping, the defects, and the length of the nanotube on the nanotube hardness are consistent with the effect of these same structural parameters on the bandgap. The *armchair* nanotubes with zipper defects are perceived as the most reactive nanotubes and the ones having the best conductive ability enhanced by nitrogen doping and longer nanotubes.

Softness, S, is the reciprocal of hardness. A larger value of softness indicates greater ability to hold a charge once acquired by the nanotube. For *armchair* (5,5) nanotubes of 16 cl, the softness varies between 0.87 and 2.06 eV and grows with the defects and with the number of defects. Nitrogen-doped nanotubes have a value of S greater than nondoped nanotubes. The only exception is for nanotubes with one SW defect (see **Table 4**).

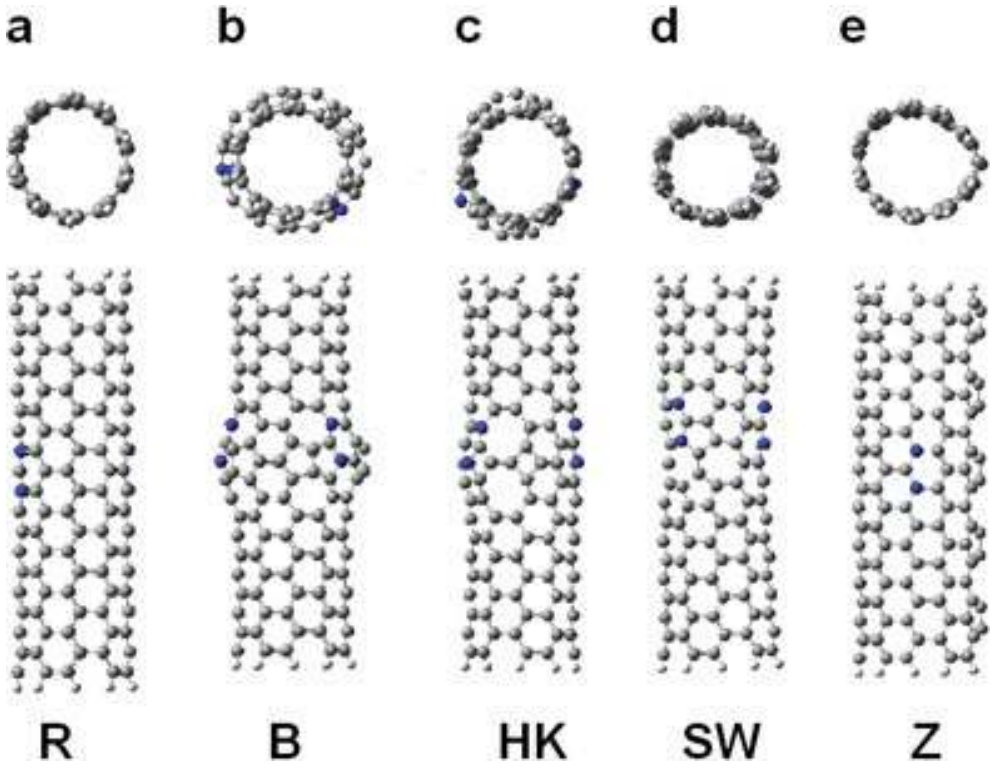


**Figure 7.** B3LYP/6-31G(d) fully optimized structures of nitrogen-doped *armchair* nanotubes. Front and lateral views showing (a) regular, R; (b) bumpy B, with five defects; (c) haeckelite HK, with two defects; (d) Stone-Wales SW, with two defects; and (e) zipper Z, with five defects, nanotubes with 20 cl of length each.

### 5.4. Electrophilicity index

The *armchair* (5,5) nanotubes of 16 cl exhibit an ω value of 11.32 eV. The presence of defects in these nanotubes increases the value of ω. The highest value of ω corresponds to the nanotubes with a SW defect (25.78 eV). Nitrogen doping also increases the ω value for regular and defective (5,5) and (6,6) nanotubes except for nanotubes with one SW defect (see **Table 4** and **Figure 5**). The (5,5) nanotubes of 20 cl show the same trend regarding the presence of defects and the nitrogen doping, being highlighted the nanotubes with zipper defects that show the highest values of ω of 27.72 and 25.94 eV for the nondoped and doped nanotubes, respectively (see **Figures 6** and **7**). These high ω values show the great tendency of these nanotubes to acquire electronic density and their high ability to be reduced compared to the other studied nanotubes. This property of *armchair* nanotubes with zipper defects, coupled with their high reactivity and good conductive ability, opens a range of possibilities as advanced materials in the field of electronics or other fields where good electrophiles or catalysts are required in redox reactions.

### 5.5. Charges

A possible explanation for the reactivity of *armchair* nanotubes with zipper defects may be the charge that develops at the C2 carbon atom that is adjacent to both pyrimidine nitrogen atoms. It has been found to be a feature that allows nitrogen-doped CNTs to behave as good catalysts [11, 12]. Our calculations reveal that the C2 carbon atom Mulliken charge on the nitrogen-doped *armchair* nanotubes with zipper defects reaches a high value of 0.26 *e*, compared with 0.01 *e* for the corresponding nondoped nanotubes. In *armchair* nanotubes with bumpy defects, this charge has a value of 0.14 *e*.

Our results, obtained using the DFT methods, contribute with a ranking of molecular structures of carbon nanotubes according to: (1) their conductive properties, (2) their hydrogen adsorption properties, and (3) their reactivity to charge transfer reactions and redox reactions. We believe that these results will help in the selection of different nanotube structures to be used in a variety of applications that consider materials such as: (1) new polymer composites having conductive properties (biodevices technology); (2) electronic devices (an electronic tongue); (3) energy storage devices; (4) suitable surface functionalized nanotubes for environmental remediation; (5) organic semiconductor-carbon nanotubes composites for separation technology (water purification); (6) catalyst for oxygen reduction reactions; (7) drug delivery systems, imaging and photothermal therapy (biomedicine); and others where tailoring of particular nanotube molecular properties is required.

## 6. Conclusions

We have performed a systematic study of the reactivity of carbon nanotubes based on various structural parameters by using molecular descriptors obtained by the DFT methods at the B3LYP/6-31G(d) level. Our results confirm that the reactivity of nanotubes depends on their structure. The chirality, the diameter, and the presence of structural, topological, and doping defects significantly modify the reactivity of the nanotubes. The *zigzag* nanotubes, both the regular (defect free) and those with bumpy defects, reveal greater reactivity, better conductive ability, and better behavior as good electrophiles when compared with corresponding *armchair* and *chiral* nanotubes suggesting a high ability to be reduced. Within the *armchair* nanotubes, we highlight those with zipper defects over those with bumpy, haeckelite, and Stone-Wales defects. The *armchair* nanotubes with zipper defects are revealed to be more reactive, with high conductive capacity, good ability to acquire electronic density and to behave as good electrophiles, and potential good catalysts in redox reactions. Nitrogen doping reveals as an important parameter that increases the conductive ability and reactivity of *armchair* nanotubes of different diameter and length. Saturated nanotubes behave as less reactive than unsaturated nanotubes. Saturated *armchair* nanotubes with bumpy defects exhibit favorable values of the hydrogen physisorption energy suggesting a reversible hydrogen adsorption-desorption process at ambient conditions.

These results are valuable to increase the understanding about carbon nanotubes activity and to contribute to the future design of novel useful materials.

To expand the range of applications of carbon nanotubes, an interesting future contribution would be to construct a nanotube-scale of reactivity, based on the values of some reactivity descriptors and their relation with experimental values for some known reactions. The aim of predicting the reactivity of different structures of nanotubes or to be able to designing nanostructures that possess a desired property to obtain advanced materials in a rational way is open.

## Acknowledgements

The authors thank the support of both the Scientific and Technological Direction and the Technological Development Society of the University of Santiago de Chile, Usach, Projects 061642CF and CIA 2981, and the computational resources at the central cluster of the Faculty of Chemistry and Biology. They also thank Mr. Ignacio Villarroel for his valuable technical assistance.

## Author details

María Leonor Contreras Fuentes* and Roberto Rozas Soto

*Address all correspondence to: leonor.contreras@usach.cl

Computational Chemistry and Intellectual Property Laboratory, Department of Environmental Sciences, Faculty of Chemistry and Biology, University of Santiago de Chile, USACH, Santiago, Chile

## References

[1] Smithells RW, Newman CGH. Recognition of thalidomide defects. Journal of Medical Genetics. 1992;**29**:716-723. Available from: http://www.thalidomide.ca/recognition-of-thalidomide-defects/ [Accessed: 19-07-2017]

[2] Dekker C. Carbon nanotubes as molecular quantum wires. Physics Today. 1999;**52**(5): 22-28. DOI: 0.1063/1.882658

[3] Pastorin G. Crucial functionalizations of carbon nanotubes for improved drug delivery: A valuable option? Pharmaceutical Research. 2009;**26**(4):746-769. DOI: 10.1007/s11095-008-9811-0

[4] Lu X, Chen Z. Curved pi-conjugation, aromaticity, and the related chemistry of small fullerenes ($C_{60}$) and single-walled carbon nanotubes. Chemical Reviews. 2005;**105**(10): 3643-3696. DOI: 10.1021/cr030093d

[5] Das D, Rahaman H. Carbon Nanotube and Graphene Nanoribbon Interconnects. New York: CRC Press Taylor & Francis Group; 2015. 196 p 9781138822313

[6] Tour JM, Dyke CA, Flatt AK. Bulk separation of carbon nanotubes by bandgap. 2011. US Patent Nr 7,939,047

[7] Howe WR, Hunt JH, Li AW. Nanotube signal transmission system. 2015. US Patent Nr 9,086,523

[8] Huang Y, Fan CQ, Dong H, Wang SM, Yang XC, Yang SM. Current applications and future prospects of nanomaterials in tumor therapy. International Journal of Nanomedicine. 2017;**12**:1815-1825. DOI: 10.2147/IJN.S127349

[9] Yu J, Zhou W, Xiong T, Wang A, Chen S, Chu B. Enhanced electrocatalytic activity of Co@N-doped carbon nanotubes by ultrasmall defect-rich $TiO_2$ nanoparticles for hydrogen evolution reaction. Nano Research. 2017;**10**(8):2599-2609. DOI: 10.1007/s12274-017-1462-1

[10] Terrones M. Synthesis toxicity and applications of doped carbon nanotubes. Acta Microscópica. 2007;**16**(1–2):33-34. Available from: https://www.ciasem.com/PSD/Cusco2007/images-1/Terrones.pdf [Accessed: 26-07-2017]

[11] Gong KP, ZH D, Xia ZH, Durstock M, Dai LM. Nitrogen-doped carbon nanotube arrays with high electrocatalytic activity for oxygen reduction. Science. 2009;**323**:760-764. DOI: 10.1126/science.1168049

[12] Hu X, Zhou Z, Lin Q, Wu Y, Zhang Z. High reactivity of metal-free nitrogen-doped carbon nanotube for the C—H activation. Chemical Physics Letters. 2011;**503**:287-291. DOI: 10.1016/j.cplett.2011.01.045

[13] Contreras ML, Villarroel I, Rozas R. Hydrogen physisorption energies for bumpy, saturated, nitrogen-doped single-walled carbon nanotubes. Structural Chemistry. 2016;**27**(5):1479-1490. DOI: 10.1007/s11224-016-0767-0

[14] Singh AK, Yakobson BI. First principles calculations of H-storage in sorption materials. Journal of Materials Science. 2012;**47**:7356-7366. DOI: 10.1007/s10853-012-6551-7

[15] Brozena AH, Leeds JD, Zhang Y, Fourkas JT, Wang Y. Controlled defects in semiconducting carbon nanotubes promote efficient generation and luminescence of trions. ACS Nano. 2014;**8**(5):4239-4247. DOI: 10.1021/nn500894p

[16] Zhu J, Childress AS, Karakaya M, Dandeliya S, Srivastava A, Lin Y, Rao AM, Podila R. Defect-engineered graphene for high-energy- and high-power-density supercapacitor devices. Advanced Materials. 2016;**28**(33):7185-7192. DOI: 10.1002/adma.201602028

[17] Contreras ML, Avila D, Alvarez J, Rozas R. Computational algorithms for fast-building 3D carbon nanotube models with defects. Journal of Molecular Graphics and Modelling. 2012;**38**:389-395. DOI: 10.1016/j.jmgm.2012.05.001

[18] Hypercube Inc. HyperChem Release 7.5. Gainesville; 2003

[19] Becke AD. Density-functional thermochemistry. The role of exact exchange. The Journal of Chemical Physics. 1993;**98**:5648-5652. DOI: 10.1063/1.464913

[20] Lee C, Yang W, Parr RG. Development of the Colle-Salvetti correlation-energy formula into a functional of the electron density. Physical Review B. 1988;**37**:785-789. DOI: 10.1103/PhysRevB.37.785

[21] Schrôdinger LLC. Jaguar version 9.2. New York; 2013

[22] Grimme S, Antony J, Ehrlich S, Krieg H. A consistent and accurate ab initio parametrization of density functional dispersion correction (DFT-D) for the 94 elements H-Pu. The Journal of Chemical Physics. 2010;**132**(15):154104. DOI: 10.1063/1.3382344

[23] Hujo W, Grimme S. Performance of the van der Waals density functional VV10 and (hybrid)GGA variants for thermochemistry and noncovalent interactions. Journal of Chemical Theory and Computation. 2011;**7**(12):3866-3871. DOI: 10.1021/ct200644w

[24] Vydrov OA, Van Voorhis TJ. Nonlocal van der Waals density functional: The simpler the better. The Journal of Chemical Physics. 2010;**133**:244103. DOI: 10.1063/1.3521275

[25] Contreras ML, Cortés-Arriagada D, Villarroel I, Alvarez J, Rozas R. Evaluating the hydrogen chemisorption and physisorption energies for nitrogen-containing single-walled carbon nanotubes with different chiralities: A density functional theory study. Structural Chemistry. 2014;**25**(4):1045-1056. DOI: 10.1007/s11224-013-0377-z

[26] DiLabio GA, Koleini M, Torres E. Extension of the B3LYP–dispersion-correcting potential approach to the accurate treatment of both inter- and intra-molecular interactions. Theoretical Chemistry Accounts. 2013;**132**:1389. DOI: 10.1007/s00214-013-1389-x

[27] Parr RG, Pearson RG. Absolute hardness: Companion parameter to absolute electronegativity. Journal of the American Chemical Society. 1983;**105**:7512-7516. DOI: 10.1021/ja00364a005

[28] Koopmans T. Über die zuordnung von wellenfunktionen und eigenwerten zu den einzelnen elektronen eines atoms. Physica. 1934;**1**:104-113. DOI: 10.1016/S0031-8914(34)90011-2

[29] Kohn W, Sham LJ. Self-consistent equations including exchange and correlation effects. Physical Review B. 1965;**140**:A1133-A1138. DOI: 10.1103/PhysRev.140.A1133

[30] Parr RG, Yang W. Density-functional theory of the electronic structure of molecules. Annual Review of Physical Chemistry. 1995;**46**:701-728. DOI: 10.1146/annurev.pc.46.100195.003413

[31] Parr RG, von Szentpaly L, Liu S. Electrophilicity index. Journal of the American Chemical Society 1999;**121**:1922-1924. DOI: 10.1021/ja983494x

[32] Toro-Labbé A. Characterization of chemical reactions from the profiles of energy, chemical potential, and hardness. The Journal of Chemical Physics A. 1999;**103**(22):4398-4403. DOI: 10.1021/jp984187g

[33] Gómez-Jeria JS. A new set of local reactivity indices within the Hartree-Fock-Roothaan and density functional theory frameworks. Canadian Chemical Transactions. 2013;**1**:25-55. DOI: 10.13179/canchemtrans.2013.01.01.0013

[34] Domingo LR, Ríos-Gutiérrez M, Pérez P. Applications of the conceptual density functional theory indices to organic chemistry reactivity. Molecules. 2016;**21**:748-769. DOI: 10.3390/molecules21060748

[35] Domingo LR, Aurell MJ, Pérez P, Contreras R. Quantitative characterization of the global electrophilicity power of common diene/dienophile pairs in Diels-Alder reactions. Tetrahedron. 2002;**58**:4417-4423. DOI: 10.1016/S0040-4020(02)00410-6

[36] Dillon AC, Jones KM, Bekkedahl TA, Kiang CH, Bethune DS, Heben MJ. Storage of hydrogen in single-walled carbon nanotubes. Nature. 1997;**386**(6623):377-379. DOI: 10.1038/386377a0

[37] Alonso JA, Arellano JS, Molina LM, Rubio A, Lopez MJ. Interaction of molecular and atomic hydrogen with single-wall carbon nanotubes. IEEE Transactions on Nanotechnology. 2004;**3**(2):304-310. DOI: 10.1109/TNANO.2004.828678

[38] Bilic A, Gale JD. Chemisorption of molecular hydrogen on carbon nanotubes: A route to effective hydrogen storage? The Journal of Physical Chemistry C. 2008;**112**:12568-12575. DOI: 10.1021/jp802104n

[39] Yao Y. Hydrogen storage using carbon nanotubes. In: Marulanda JM, editor. Carbon Nanotubes. 2010. In-the:India. p. 543-562. DOI: 10.5772/39443

[40] Kovalev V, Yakunchikov A, Li F. Simulation of hydrogen adsorption in carbon nanotube arrays. Acta Astronautica. 2011;**68**:681-685. DOI: 10.1016/j.actaastro.2010.09.007

[41] Liu C, Chen Y, CZ W, ST X, Chen HM. Hydrogen storage in carbon nanotubes revisited. Carbon. 2010;**48**:452-455. DOI: 10.1016/j.carbon.2009.09.060

[42] Contreras ML, Rozas R. Nitrogen-containing carbon nanotubes—A theoretical approach. In: Bianco S, editor. Carbon Nanotubes. From Research to Applications. Croatia: InTech; 2011. p. 3-26. DOI: 10.5772/16946 Available from: http://www.intech.open.com/books/carbon-nanotubes-from-research-to-applications/nitrogen-containing-carbon-nanotubes-a-theoretical-approach

[43] Ghosh S, Padmanabhan V. Adsorption of hydrogen on single-walled carbon nanotubes with defects. Diamond & Related Materials. 2015;**59**:47-53. DOI: 10.1016/j.diamond.2015.09.004

[44] Tabtimsai C, Keawwangchai S, Nunthaboot N, Ruangpornvisuti V, Wanno B. Density functional investigation of hydrogen gas adsorption on Fe-doped pristine and Stone-Wales defected single-walled carbon nanotubes. Journal of Molecular Modeling. 2012;**18**(8):3941-3949. DOI: 10.1007/s00894-012-1388-1

[45] Gayathri V, Geetha R. Hydrogen adsorption in defected carbon nanotubes. Adsorption. 2007;**13**(1):53-59. DOI: 10.1007/s10450-007-9002-z

[46] Meng FY, Zhou LG, Shi SQ, Yang R. Atomic adsorption of catalyst metals on Stone–Wales defects in carbon nanotubes. Carbon. 2003;**41**:2009-2025. DOI: 10.1016/S0008-6223(03)00183-0

[47] Shevlin SA, Guo ZX. High-capacity room-temperature hydrogen storage in carbon nanotubes via defect-modulated titanium doping. The Journal of Physical Chemistry C. 2008;**112**:17456-17464. DOI: 10.1021/jp800074n

[48] Simeon T, Balasubramanian K, Welch CR. Theoretical study of the interactions of $In^{+}$ and $In^{3+}$ with Stone-Wales defect single-walled carbon nanotubes. The Journal of Physical Chemistry Letters. 2010;**1**:457-462. DOI: 10.1021/jz900125e

[49] Targets for onboard hydrogen storage systems for light-duty vehicles. 2009. Available from: http://www.eere.energy.gov/hydrogenandfuelcells/storage/pdfs/targets_onboard_hydro_storage_explanation.pdf. [Accessed 2017–07-24]

[50] Li J, Furuta T, Goto H, Ohashi T, Fujiwara Y, Yip S. Theoretical evaluation of hydrogen storage capacity in pure carbon nanostructures. The Journal of Chemical Physics. 2003; **119**:2376. DOI: 10.1063/1.1582831

[51] Lochan RC, Head-Gordon M. Computational studies of molecular hydrogen binding affinities: The role of dispersion forces electrostatics and orbital interactions. Physical Chemistry Chemical Physics. 2006;**8**:1357-1370. DOI: 10.1039/B515409J

[52] Panczyk T, Wolski P, Lajtar L. Coadsorption of doxorubicin and selected dyes on carbon nanotubes. Theoretical investigation of potential application as a pH-controlled drug delivery system. Langmuir. 2016;**32**:4719-4728. DOI: 10.1021/acs.langmuir.6b00296